Experimental methods for studying spontaneous and low-energy nuclear fission

G. M. Ter-Akop'yan, Yu. Ts. Oganesyan, A. V. Daniel', and G. S. Popeko
Joint Institute for Nuclear Research, Dubna

J. Hamilton, J. Kormicki, and A. Ramayya
Department of Physics and Astronomy, Vanderbilt University, Nashville, TN

J. Kliman
Institute of Physics, Slovak Academy of Sciences, Bratislava, Slovak Republic

J. Rasmussen
Lawrence Berkeley National Laboratory, Berkeley, CA

Fiz. Élem. Chastits At. Yadra **28**, 1357–1388 (November–December 1997)

The various experimental methods used in studying spontaneous and low-energy nuclear fission in order to determine the fragment kinetic energy, mass, charge, excitation energy, and spin are reviewed. Special attention is paid to the description of a new approach to the study of fission based on the spectrometry of multiple prompt fission γ rays. Some new data on the spontaneous fission of ^{252}Cf obtained using this approach are presented. © *1997 American Institute of Physics.* [S1063-7796(97)00106-X]

INTRODUCTION

Nuclear fission was discovered more than half a century ago. Since then, an enormous amount of experimental data has been accumulated. The analysis of the data has led to the discovery and understanding of fundamental regularities of nuclear fission.[1] There is a deep connection among the values of the total kinetic energy (TKE), the mass asymmetry, and the excitation energy of fragments from spontaneous and low-energy nuclear fission. These parameters are mainly determined by the scission configuration of the nucleus. After the nucleus splits, the Coulomb interaction energy is transformed into the kinetic energy of the produced fragments, while the deformation energy becomes the excitation energy.

In the multidimensional deformation space the potential energy of the cold nucleus has a complicated structure determined by shell effects in the deformed nucleus. For various fissile systems the potential-energy surface has a clearly expressed valley running from the saddle points to the points of the most probable nuclear scission.[2–6] The fission process evolves along these valleys. The various fission paths of the nucleus in deformation space are called the fission channels or modes. Each fission mode is characterized by the average mass of the fragments, the mass variance, the average TKE, and the variance of the TKE.[7–9] The model of multiplicative fission based on analysis of the potential-energy surface of the deformed nucleus allows the successful prediction of the average values of the fragment masses and average TKE for various fission channels. Explanation of the variances in the mass and energy distributions of the fission fragments requires study of not only the nuclear potential energy, but also the dynamics of the fission process. A combination of the multichannel fission model and the model of random breaking of the nuclear neck based on the assumption that a dynamical instability arises in this breaking allows the mass and energy distributions of the fragments of spontaneous and low-energy fission to be interpreted successfully.[10]

As the nuclear shape evolves from the saddle point to the scission point, the energy released ΔV is partially transformed into kinetic energy, the so-called prefission kinetic energy of the fragments. Another part of the energy ΔV goes into the excitation of the collective degrees of freedom of the nucleus (dipole oscillations and oscillations in the direction perpendicular to the fission axis) and, when nuclear viscosity is present, part of ΔV will go into the internal energy of the fissioning nucleus. At present there are few experimental data which can be used to estimate the distribution of the energy release ΔV and to extract information about the dynamics of nuclear fission. The experimental data are clearly insufficient for constructing a systematic model of the fission dynamics, and the existing models which succeed in explaining various specific features of the dynamics give contradictory results.

Detailed studies of the isobar distributions of fragments (the yields of fragments with various charges Z at fixed mass A) have led to a new understanding of several aspects of the fission process associated with the dynamics. Study of the variances of the isobar distributions (σ_Z^2; Ref. 11) has led to the establishment of a connection between the formation of the fragment charge distributions and the zero-point dipole oscillations of a harmonic oscillator.[12] According to this model, before the nuclear scission, when the neck radius becomes small the process becomes nonadiabatic, and the charge variance of the fragments is determined by the rate at which the neck breaks.[13] The experimental values of σ_Z^2 for various fissile systems are reproduced by this model when the neck-breaking rate is $\simeq 2$ F/10^{-21} sec. However, the behavior of the average charges of the isobar distributions of fission fragments (polarization of the fragment charges) as a function of the fragment mass, which has been observed in the fission of actinide nuclei from Th to Cf, is still not understood.

Study of the properties of the proton even–odd effect, i.e., the excess in the yield of fragments with even charge

over the yield of fragments with odd charge, for various fissile systems[11,14,15] has given some information about the nuclear excitation energy as scission is approached. On the basis of calculations of the magnitude of the even–odd effect by combinatorial analysis of the number of broken proton pairs,[16] it has been estimated that the dissipation energy is about 30% of ΔV (Ref. 17). However, this estimate is usually viewed as an upper limit on the dissipation energy, because pair scission during the rapid nonadiabatic breaking of the nuclear neck was neglected in the calculations.[18]

An interesting manifestation of the nuclear fission dynamics is the fact that some of the fragments of spontaneous and low-energy fission have angular momenta considerably larger than the spin of the fissioning nucleus. The fragment angular momentum has been attributed to the excitation of transverse oscillations in the fissioning nucleus as it moves from the saddle point to the scission point. Starting from the assumption of statistical equilibrium at the scission point, theoretical studies[19,20] have shown that the fragment angular momentum must increase as the fragment deformation increases at the scission point. However, the fragment angular momenta and their relation to other characteristics of spontaneous and low-energy nuclear fission are poorly studied.

Thus, in fission physics there are several problems associated with the dynamics of the fission process whose solution requires new, more detailed experimental studies of the fission characteristics. Such new data can be obtained both by improving the experimental techniques and existing methods of study, and by new approaches to studying fission. In this review we shall discuss the experimental techniques for studying low-energy and spontaneous nuclear fission. In Sec. 1 we briefly review the existing methods used to determine the various characteristics of nuclear fission. Special attention is paid to the description of a new, original method of studying fission, which is the subject of Sec. 2. This method has been proposed and realized in our studies on the spontaneous fission of ^{252}Cf.[21–30]

1. PHYSICAL METHODS OF DETERMINING THE CHARACTERISTICS OF NUCLEAR FISSION

Every fission event is characterized by the mass, charge, kinetic energy, excitation energy, and spin of the two fragments. A special feature of the fission process is the broad spectrum of states of the produced fragments. The characteristics of the distributions of the observed fission properties and the correlations between them contain information about the features and regularities of the fission process, and also about the properties of nuclear matter which are manifested in large-amplitude collective motion.

1.1. The fragment masses

Most of the data on the mass distributions of the fragments of low-energy and spontaneous fission have been obtained by measuring the kinetic energy of the fragment pairs in so-called $(2E)$ experiments. The fragment mass distributions in fission are determined by using the relation between the fragment kinetic energy and mass following from the conservation laws in binary low-energy nuclear fission. For primary fragments (before nucleon evaporation) the sum of the fragment masses A_i is equal to the mass of the fissioning nucleus A_F:

$$A_1+A_2=A_F.$$

This relation is valid for the overwhelming majority of spontaneous and low-energy fission events, because cases where neutrons are emitted from the nucleus before fission are very rare. For example, in the spontaneous fission of ^{252}Cf, as shown in Ref. 31, neutrons are emitted from fully accelerated fragments.

In spontaneous fission and also in fission induced by thermal neutrons, when the transferred momentum is negligible compared with the fragment momenta, we have

$$A_1v_1=A_2v_2. \tag{1}$$

This leads to an expression for the fragment kinetic energies:

$$E_1/E_2=A_2/A_1, \tag{2}$$

where E_i is the kinetic energy of a primary fragment. Knowing the fragment energies, it is possible to find the mass of each fragment:

$$A_1=A_F\cdot E_2/(E_1+E_2). \tag{3}$$

However, it should be remembered that Eqs. (1)–(3) are valid for primary fragments, when neutrons are not evaporated from the fragments. This occurs only in about 1% of cases of nuclear fission. In the other cases neutrons are emitted from the moving fragments. Therefore, a fragment reaching the detector has mass A_i' and kinetic energy E_i' different from the initial values:

$$A_i'=A_i-\bar{\nu}_i, \tag{4}$$

where $\bar{\nu}_i$ is the average number of neutrons emitted from a fragment of mass A_i. Assuming that the neutrons are evaporated with zero velocity relative to the fragment, it is easy to obtain the following relation between the energies of the primary and secondary fragments:

$$E_i'=E_i(A_i-\bar{\nu}_i)/A_i. \tag{5}$$

To determine the kinetic energy and mass of the primary fragments it is necessary to introduce corrections associated with neutron evaporation. The average number of evaporated neutrons is a function of the fragment mass. These functions are known for several thermal-neutron induced fission reactions and for nuclei which undergo spontaneous fission. The fragment masses and energies are calculated by the standard procedure.[32]

The kinetic energy of a fragment E' after neutron evaporation will not only be shifted relative to the initial fragment energy [see Eq. (5)], but will also be smeared about the average energy $\langle E'\rangle$ with width $\sigma(E')$, owing to the variation of the number of evaporated neutrons and the momentum carried off by them. Therefore, the fragment masses obtained in $(2E)$ experiments can be determined with an error which is due to the fission process itself. The author of Ref. 33 made a careful analysis of the mass resolution which can be obtained for fragments in $(2E)$ experiments. For the stan-

dard reaction $^{235}U(n_{th},f)$ and the spontaneous fission of ^{252}Cf, the calculated mass resolutions are, respectively, $\delta A=3$ amu for ^{235}U and $\delta A=4$ amu for ^{252}Cf. The method of determining the fragment mass using the kinetic-energy ratio of the secondary fragments does not in principle allow the determination of the fragment masses with an accuracy better than this.

The energies of fragment pairs are usually measured by using two types of detector: pulse ionization chambers (ICs) and silicon detectors (SDs). Most of the available data on nuclear fission have been obtained by using SDs, because these detectors are compact and do not require a high-voltage power supply and thus are simple and convenient to use. To transform the pulse height given by the detector when it records a fragment into the fragment energy it is necessary to take into account the amplitude defect. In an SD this is mainly determined by the ionization defect and incomplete collection of charge carriers. It has been established experimentally that the pulse height depends linearly on the energy of fixed-mass fragments. The calibration function relating the pulse height N to the energy E of a fragment of mass A is written as

$$E=(a+b\cdot A)\cdot N+c+d\cdot A,$$

where a, b, c, and d are constant coefficients determined individually for each detector from the energy spectra of the best-studied fission reactions $^{235}U(n,f)$ and ^{252}Cf(s.f.), using the parametrization of the fragment energy spectra proposed in Ref. 34.

The fragment energy resolution which can be obtained using an SD is 1–2 MeV (Ref. 35). The mass resolution obtained in $(E2)$ experiments is usually 4–5 mass units.[36]

Gas-filled ionization chambers have been used successfully in recent years to study fission. Such chambers are interesting, owing to the flexibility in the chamber construction, the absence of radiation damage, and the significantly better energy resolution than for silicon detectors. Double ionization chambers with planar electrodes separated by a common cathode are most convenient for studying spontaneous fission or neutron-induced fission.[37,38]

The amplitude defect of ICs is mainly determined by the ionization defect and energy loss in the backing (or in the entrance window, if an external source is used). The angle at which the fragment enters the IC is measured in order to correctly take into account the energy loss in the backing. The entrance angle is determined by the ionization chamber itself, for example, from the ratio of the anode and cathode signals.

The fragment energy resolution obtained in an IC is 0.4 and 0.5 MeV, respectively, for light and heavy fragments.[39] The mass resolution for $(2E)$ experiments using ICs is usually 3–4 mass units. A double ionization chamber has been used for a careful study of the phenomenon of cold nuclear fission.[40–42] In cold fission the fragments do not emit neutrons, and almost all the fission energy is transformed into kinetic energy of the fragments. The mass distribution measured in cold fission is determined only by the energy resolution of the chamber, according to Eq. (3).

The fragment mass distribution can also be obtained by measuring the velocities of fragment pairs in $(2V)$ experiments. Knowing the mass of the fissioning nucleus A_F, it is possible to find the fragment masses and energies:

$$A_1=A_F\cdot v_2/(v_1+v_2), \tag{6}$$

$$E_i=A_i\cdot v_i^2/2. \tag{7}$$

Equations (6) and (7) can be used to calculate the total kinetic energy of the primary fragments: $\mathrm{TKE}=A_F\cdot v_1\cdot v_2/2$. The fragment energies obtained by measuring the velocities do not require energy calibration. This method gives the absolute values of the kinetic energy.

Since neutron emission is isotropic in the fragment rest frame, the value of the average fragment velocity after neutron evaporation does not change. The velocities measured experimentally and the values of the mass and energy obtained using Eqs. (6) and (7) pertain to the primary fragments. The velocity spread due to neutron emission leads to a spread in the calculated fragment masses. As shown in Ref. 33, the mass spread in $(2V)$ experiments is smaller than the mass spread in $(2E)$ experiments. In $(2V)$ experiments the mass spread is $\delta A=1.4$ amu for the reaction $^{235}U(n_{th},f)$ and $\delta A=1.9$ amu for the spontaneous fission of ^{252}Cf. Thus, the two methods of determining the fragment mass in $(2E)$ and $(2V)$ experiments in principle do not allow the unique determination of the fragment mass numbers.

The fragment velocity is determined by measuring the time T to travel a given distance d. Detectors which mark the time at the beginning and end of the passage of a fragment over a baseline d must have good time resolution. Since the fragment velocity is of order 10^9 cm/sec, for a baseline of 1 m it is necessary to have a time resolution of at least 10^{-9} sec in order to obtain a mass resolution of $\delta A/A=1\%$. In addition, the first detector must be thin enough that the fragment speed changes only insignificantly in passing through it.

The best time resolution is obtained by using detectors which record emission electrons, and so such detectors are used most often in experiments. Thin ($10–20\ \mu g/cm^2$) carbon or alundum films are used for electron emission. The electron yield is determined by the specific ionization energy losses, and for fission fragments it reaches several hundred. To obtain good time resolution, it is important to ensure that the electron motion from the production region to the detector is isochronous. This is achieved, first, by increasing the electron velocity. The average energy of the emission electrons is several eV. Before detection the electrons are accelerated in an electric field to an energy of several keV. Second, migration of the electrons toward the detector is ensured by a uniform magnetic field or an electrostatic mirror so as to obtain trajectories of identical lengths. Microchannel plates are used as the electron detector. This method ensures 100% efficiency in recording fission fragments. A time resolution better than $\delta T=100$ psec is obtained for a system consisting of two such detectors which measures the fragment time of flight.[43] Thin plastic scintillators with a time resolution of $\delta T\geqslant 200$ psec are also used for time marking.[44]

The fragment time of flight is also measured by using parallel-plate avalanche counters (PPACs).[45] Avalanche counters have good time resolution (100–200 psec) and record fission fragments with 100% efficiency. PPACs can also be used as ΔE detectors. The minimum matter thickness traversed by fragments in a PPAC is 200–300 μg/cm^2 (scaled to carbon), which makes it difficult to use these counters to obtain a start signal. PPACs of large area are used as detectors of stop signals in order to increase the geometrical efficiency of fragment detection. These PPACs are made to be position-sensitive in order to take into account change of the baseline. The particle point of passage can be determined with an error of about 0.5 mm.

The technique of determining the fragment mass by simultaneously measuring the fragment velocity (or momentum) and energy [the (E,V) method] provides a mass resolution as good as that of radiochemical methods. It should be stressed that when the energy and velocity of a single fragment are measured it is possible to obtain the mass of only secondary fragments. The energy and momentum of a charged particle can be determined very accurately from the deflection of the particle trajectory in electric and magnetic fields. Electromagnetic spectrometers are used successfully to study fission fragments. For example, the Lohengrin spectrometer with double focusing developed at the high-flux reactor in Grenoble permits the mass separation of both heavy and light fragments with a resolution of better than $\delta A/A = 2\times 10^{-3}$. The energy resolution is $\delta E/E = 2\times 10^{-3}$.

Modern detectors can be used to obtain the same mass resolution as with mass spectrometers. In fact, since $A = 2E/v^2$ and $v = d/T$, where d is the baseline and T is the corresponding time, the mass resolution of the (E,V) method is given by

$$\delta A/A = [(\delta E/E)^2 + (\delta T/T)^2]^{1/2}.$$

We see from this expression that a resolution of one mass unit cannot be obtained in measuring the fragment energy by a silicon detector, because the energy resolution of these detectors is no better than 2%. The energy resolution of ionization chambers allows fragments with adjacent mass numbers to be distinguished. A mass resolution of $\delta A = 0.6$ amu was obtained in Ref. 43 for light fragments. In these experiments the fragment energy was measured by a gas-filled ionization chamber, and the velocity was measured by a time-of-flight detector.

1.2. The nuclear charge of the fragments

To identify a fission fragment, it is important to know not only the fragment mass, but also its nuclear charge. For a long time, radiochemical methods were not viewed as a practical way of measuring the charge. However, recently the experimental technique has developed to the point where a great deal of important experimental information has been obtained about the fragment charge distributions.

Let us consider the possibilities offered by various methods of determining the nuclear charge. The simplest is measurement of the fragment charge using K x rays.[46] In fact, high-resolution γ detectors allow the fragment charge to be determined using K x rays without mass separation of the fragments. The difficulty is that the x-ray yield depends on the nuclear structure of the fragments. Since this dependence is not well understood, this method is not widely used. Nevertheless, the element yield of fragments from the spontaneous fission of ^{252}Cf found using x rays agrees well with the element yield measured by the $\Delta E - E$ method.[47]

In recent years, new possibilities have arisen for the identification of fragments according to their characteristic γ radiation. Owing to the development of γ spectroscopy and 4π systems of germanium detectors which record multiple γ rays with high efficiency, a large amount of information has been obtained about the structure of the rotational and quasirotational levels which are populated in the deexcitation of the fission fragments.[22,23,49–59] High-resolution γ spectroscopy allows the fragment mass and charge to be determined uniquely from the γ-ray energy. In addition, the fragment yield can be determined from the intensity of the γ radiation. It is known that the intensity of the $2^+ \rightarrow 0^+$ transition for an even–even fragment accurately corresponds to the independent yield of this fragment.[60] The technique of γ spectroscopy has been used to determine the independent yields of fragments from the spontaneous fission of ^{252}Cf (Ref. 60), and also of fragments from the thermal-neutron-induced fission of ^{235}U (Ref. 61) and ^{239}Pu (Ref. 62). The possibilities offered by the spectroscopy of multiple prompt fission γ rays for studying nuclear fission and obtaining new characteristics of the fission process will be discussed in the next section.

Various approaches based on analysis of the ionization density produced by fragments in the detector material are used to determine the fragment nuclear charge (Z). The fragments of spontaneous and low-energy nuclear fission have extremely small velocities and so do not give a Bragg peak in the ionization curve. However, the ionization curve contains information about the nuclear charge. The energy lost to ionization dE/dx for fragments stopped in a medium can be written as

$$dE/dx \sim f(Z)\cdot v, \tag{8}$$

and the fragment range in a medium is

$$R \sim M\cdot v/f(Z), \tag{9}$$

where v is the fragment velocity and $f(Z)$ is a function of the fragment charge, which for a light stopping medium ($Z > Z_{med}$) can be written as $f(Z) \sim Z^{1/6}$.

Several approaches have been developed for extracting information about the fragment charge from the ionization-loss curve. All these approaches can distinguish fragments with adjacent charges only for light fragments with charge $Z < 45$, owing to the features of the fragment ionization loss.

The fragment charge can be found by the well known $\Delta E - E_{res}$ method. The residual energy E_{res} is measured by high-resolution ionization chambers or time-of-flight detectors. Several variants of the method have been realized. Some use a passive absorber of the energy ΔE, and others use an active absorber, where the energy loss is measured by the absorber itself. For example, fragments separated in energy by the Lohengrin spectrometer have lost a part of their energy ΔE in the entrance window of the ionization chamber, and the residual energy E_{res} is measured by an ionization

chamber.[63] A nuclear-charge resolution of $\Delta Z/Z=0.02$ was obtained in these experiments for fragments with $Z=39$. A slightly different version of the $\Delta E-E_{res}$ method was used for fragments of given mass and energy separated by the Lohengrin spectrometer. The fragments also lost part of their energy in a passive absorber, but the residual energy was measured by a time-of-flight detector.[64] Thin semiconductor detectors and thin scintillators were used as the ΔE detector.[65]

The total and specific energy losses can be measured with a single ionization chamber. For this purpose, the anode is split into two parts in an ionization chamber with electric field lines perpendicular to the fragment trajectories. Some of the electrons from the track produced by the fragment are collected by the first section of the anode, and the rest are collected by the second. The value of ΔE is measured in the first part of the anode, and E_{res} is measured in the second part. For light fragments with $Z=30$ a charge resolution of $\Delta Z/Z=0.03$ was obtained with this ionization chamber.[66]

In an ionization chamber with electric field lines parallel to the fragment trajectories the shape of the Bragg ionization curve produced by a particle in the space between the cathode and the Frisch grid is reproduced by the shape of the anode signal as a function of time. The spectrometry of the Bragg curve of a gas-filled ionization chamber provides a good experimental tool for determining the charges of fission fragments. Extraction of information about the fragment charge does not require digitization of the entire Bragg curve; instead, it is sufficient to choose a suitable parameter. It follows from Eq. (9) that this can be the track length of a fragment with given mass and velocity. The track length can be determined from the time delay for the appearance of the anode signal relative to the particle time of arrival. The charge distribution obtained in this manner for fragments separated by the Lohengrin spectrometer was $\Delta Z/Z=0.025$ in the case of fragments with $Z=40$ (Ref. 39). The same method of determining the charge is used in the double time-of-flight spectrometer Cosi Fan Tutte,[14] located at a reactor with a high neutron flux. It also gave beautiful results in the study of cold fission, using a double ionization chamber.[40] A somewhat different approach for determining the fragment charge was realized in the double ionization chamber.[67] The center of gravity of the ionization arising in the stopping of a fragment in the gas of the ionization chamber was found.

1.3. The excitation energy of fission fragments

In spontaneous and low-energy nuclear fission, the fragment excitation energy is mainly determined by the deformation of the fragments at the instant when the nucleus splits. In addition, the fragments can acquire an excitation energy as a result of the heating of the fissioning nucleus as it moves from the saddle point to the scission point. The fragments produced are characterized by a significant deformation. The ratio of the fragment axes at the scission point is of order 1:2 (the deformation parameter is $\beta_2=0.65$). The dissipation of the deformation energy into internal excitation energy of the fragments occurs simultaneously with the acceleration of the fragments by the Coulomb field over a time of order 10^{-20} sec. The fragment excitation energy makes up about 15% of the entire fission energy. For example, for ^{252}Cf the average excitation energy of the two fragments is $\sim$30 MeV. The fragment deexcitation is described well by the statistical theory. First, the excited fragment evaporates neutrons. Neutron emission occurs over a time from 10^{-18} to 10^{-15} sec after breakup of the nucleus. When the fragment excitation energy becomes lower than the neutron binding energy, the further deexcitation proceeds via γ emission. Most of the γ rays are emitted by fragments $10^{-12}-10^{-10}$ sec after their formation.[68]

Neutron emission removes about 80% of the fragment excitation energy, and so study of the multiplicity of prompt fission neutrons is the main source of information about the fragment excitation energy. Most of the experiments in which prompt fission neutrons were studied have been based on direct detection of the neutrons. The neutron multiplicity has been obtained in experiments of varying degree of complexity. The most integral characteristic is $\bar{\nu}_{tot}$, the average number of neutrons emitted per fission event. For ^{252}Cf, $\bar{\nu}_{tot}=3.7676\pm0.0047$ (Ref. 69). More differential information is extracted from experiments in which the kinetic energy and/or velocity of the fragments is measured at the same time as the neutrons are detected. The multiplicity of prompt neutrons has been studied most thoroughly for the thermal-neutron-induced fission of ^{235}U (Refs. 70–73) and the spontaneous fission of ^{252}Cf (Refs. 75–81). The dependence of the average number of prompt neutrons on the fragment mass number has also been obtained for the reactions ^{233}U(n_{th},f) (Refs. 73 and 82) and ^{239}Pu(n_{th},f) (Ref. 73). To reconstruct the neutron multiplicity distributions from the experimental data, it is necessary to perform calculations taking into account the resolution time and efficiency of neutron detection by the detector using *a priori* information about the shape of the reconstructed distributions.

Organic scintillators (solid or liquid) and counters using ^{3}He are used to record neutrons. In scintillation detectors the pulses produced by prompt neutrons are separated from the pulses produced by γ rays according to the particle time of arrival in the detector using the time-of-flight technique. Liquid scintillators with the addition of gadolinium are widely used for recording fission neutrons. The isotopes ^{155}Gd and ^{157}Gd have the largest cross sections for thermal-neutron capture: 6.1×10^4 and 2.5×10^5 b, respectively. A neutron hitting the detector is thermalized in the detector material and captured by Gd. The gamma rays emitted in the reaction Gd(n,γ) activate the scintillator and induce luminescence, which is recorded by photomultipliers. Thus, in such detectors the neutron pulses are separated from the γ pulses by the detector itself according to the arrival time of the signals.

The neutron multiplicity can be measured accurately by using 4π detectors with high neutron-detection efficiency. The large 4π neutron detector in Melbourne measured neutrons with an efficiency of 85% (Ref. 83). This detector has a diameter of one meter and contains 500 liters of liquid scintillator based on toluene with a 0.4% admixture of Gd.

The large 4π setup in Heidelberg measures the energy and multiplicity of prompt neutrons and γ rays from fission. The setup consists of 162 NaI crystals of thickness 20 cm.[84]

The dependence of the γ-ray multiplicity from the fission of ^{252}Cf on the fragment mass and the γ-ray energy has been studied at this setup.[85]

The multiplicity of fission neutrons has also been studied in "indirect" experiments. For example, the dependence $\bar{\nu}(A)$ for ^{252}Cf was obtained in Ref. 86, using the measured kinetic energies of two fragments and the velocity of one fragment. Similar data have been obtained by measuring the velocities of two fragments and the kinetic energy of one fragment.[87] The functions $\bar{\nu}(A)$ for the thermal-neutron-induced fission of ^{233}U and ^{235}U have been obtained in recent experiments[88] by measuring the velocities and kinetic energies of two fragments. The fragment masses before neutron evaporation were found from the measured fragment velocities, and the fragment masses after neutron evaporation were found from the kinetic energies. The average number of evaporated neutrons was defined as the difference of the fragment masses before and after neutron emission. It should be noted that in several ranges of mass numbers, the dependences $\bar{\nu}(A)$ obtained in that study differ significantly (by a factor of 1.3–2) from the analogous data obtained in classical experiments[73,82] with direct neutron detection.

The neutron multiplicity distributions for various charge distributions of the fissioning nucleus can be obtained in experiments studying prompt coincident fission γ rays. We shall say more about this in the next section.

The fragment excitation energy $E_x(A)$ can be estimated from the expression

$$E_x(A)=\bar{\nu}(A)\cdot[S_n(A,Z)+\bar{\eta}(A)]+\bar{E}_\gamma(A), \qquad (10)$$

where $\bar{\nu}(A)$ and $\bar{\eta}(A)$ are the average number of neutrons and the average neutron kinetic energy, and $\bar{E}_\gamma(A)$ is the total energy carried off by the emitted γ rays. The quantity $S_n(A,Z)$, the neutron separation energy for a fragment of mass A and charge Z, can be obtained from mass tables[89] for the most probable charge of fragments of mass A. The dependences of the average neutron kinetic energy and the total energy carried off by γ rays on the fragment mass for ^{252}Cf are given in the literature (Refs. 31 and 90). The energy $\bar{E}_\gamma(A)$ carried off by the emitted γ rays can be taken into account using the relation found in Ref. 90 between the total γ energy and the number of evaporated neutrons: $\bar{E}_\gamma(A)=\bar{\nu}(A)\cdot 0.75+2$ (MeV) for the spontaneous fission of ^{252}Cf and $\bar{E}_\gamma(A)=\bar{\nu}(A)\cdot 1.1+1.75$ (MeV) for the reaction ^{235}U(n,f). For a rough estimate of the fragment excitation energy it is sufficient to know that $E_x(A)\simeq\bar{\nu}(A)\cdot 8$ MeV.

1.4. The angular momenta of fission fragments

It is well known that the fragments produced in low-energy and spontaneous nuclear fission have angular momentum considerably larger than that of the fissioning nucleus. For example, in the case of the spontaneous fission of ^{252}Cf the average angular momentum of a single fragment is (7–8)$\hbar$. The fact that the fragments from low-energy and spontaneous nuclear fission possess angular momentum is related to the fission dynamics. As the nucleus moves from the saddle point to the scission point, part of the energy released can be transformed into excitation of collective degrees of freedom. Some forms of nuclear-matter oscillations in the direction perpendicular to the fission axis lead to angular momenta of the produced fragments.[19,91] After the nuclear neck breaks, these oscillations cause the fragment angular momentum to be perpendicular to the fission axis. The distribution of the fragment angular momenta after scission of the nucleus can be changed slightly owing to the Coulomb interaction between the separating fragments.[19,92]

Most of the fragment angular momentum is carried off by γ emission. Therefore, the study of prompt fission γ rays can give the most complete information about the fragment angular momentum. Methods based on measurement of the anisotropy[92] and multiplicity[93] of prompt fission γ rays have been used to estimate the fragment angular momentum. Another well known method of determining the fragment angular momenta is that based on the isomeric ratios, which are measured in experiments for different isomeric pairs produced in fission.[94] This method has been used recently to obtain a great deal of new information about the angular momenta of fragments from low-energy nuclear fission.[95,96] However, the angular momenta of primary fragments calculated from the isomeric ratios depend strongly on the model used, and so it is difficult to compare the results of different experiments. Usually it is not the absolute values of the angular momenta obtained in this way which are compared, but rather how they vary. Most calculations of the angular momentum of primary fragments have been performed according to the statistical model of fragment deexcitation developed in Refs. 97 and 98.

The angular momentum of fission fragments can also be estimated by a method based on determination of the transition intensity in the deexcitation of the 2^+, 4^+, and 6^+ rotational bands of even–even fragments from the spontaneous fission of ^{252}Cf (Ref. 99). By now, detailed and accurate level schemes have been obtained for many fission fragments, and also the spins and parities of these levels have been determined. Therefore, new ways of reliably measuring the fragment angular momenta have arisen. In fact, in experiments in which γ rays are detected with good energy resolution, it is possible to find the probabilities of populating levels of the fragment rotational bands and to find the average spin of these levels $\bar{J}_\gamma(A',Z)$ for secondary fragments with charge Z and mass number $A'=A-\bar{\nu}(A)$. In fragment deexcitation most of the angular momentum is removed as a result of discrete γ transitions between levels of the rotational bands. When determining the initial angular momentum of the fragments it is necessary also to take into account the decrease of the angular momentum due to the emission of neutrons, $\bar{J}_n(A,Z)$, and statistical γ rays, $\bar{J}_{\text{stat}}(A,Z)$. The angular momentum of the primary fragments can be represented as the sum of three components:

$$\bar{J}(A,Z)=\bar{J}_\gamma(A',Z)+\bar{J}_n(A,Z)+\bar{J}_{\text{stat}}(A,Z)=\bar{J}_\gamma(A-\bar{\nu},Z)+\bar{\nu}(A,Z)\cdot\bar{j}_n+\bar{M}_{\text{stat}}(A,Z)\cdot\bar{j}_{\text{stat}}, \qquad (11)$$

where $\bar{j}_n$ is the average angular momentum carried off by an

evaporated neutron, $\bar{M}_{stat}(A,Z)$ is the average multiplicity of statistical γ rays, and $\bar{j}_{stat}$ is the average angular momentum carried off by a statistical γ ray.

Calculations using the statistical model of fragment deexcitation show that on the average the evaporation of a single neutron decreases the fragment spin by $(0.5–0.6)\hbar$, while the emission of a statistical γ ray decreases the angular momentum by $0.3\hbar$. For ^{252}Cf the average multiplicity of statistical γ rays is <1 for the entire range of fragment mass numbers.[85] Thus, if $\bar{J}_{\gamma}(A',Z)$ is determined experimentally, the angular momentum of the primary fragments can be estimated from Eq. (11).

2. STUDY OF THE SPONTANEOUS FISSION OF ^{252}Cf USING MULTIPLE γ RAYS

2.1. The spectroscopy of multiple γ rays

The possibilities offered by modern, large-scale, highly efficient 4π γ spectrometers[48] and knowledge of the schemes of nuclear levels populated in fission for a large number of fragments[22,23,49–59] allow a new approach to the study of nuclear fission based on the study of the multiple characteristic γ rays emitted by pairs of fission fragments. This approach has been used to obtain new characteristics of the spontaneous fission of ^{252}Cf: the independent yields of fragment pairs and the angular momenta of the fragments making up the various pairs.[21–30]

Measurements of the γ rays from the spontaneous fission of ^{252}Cf have been performed at the Oak Ridge National Laboratory with a setup consisting of 20 germanium detectors,[30] and at the Lawrence Berkeley National Laboratory using the initial version of the Gammasphere setup, in which the γ spectrometer consisted of 36 germanium detectors.[29] The ^{252}Cf sources were hermetically sealed, and the studied γ rays were emitted from stopped fragments. In experiments performed with 4π γ spectrometers, all events with γ multiplicity equal to two or more are accumulated event by event.

The analysis of the experimental data begins with the construction of the two-dimensional spectrum of coincident γ rays. The content of the spectrum is the number of events with recorded energies of the coincident γ rays $E_{\gamma 1}$ and $E_{\gamma 2}$. Two-dimensional $\gamma-\gamma$ coincidence spectra can contain several tens of thousands of peaks, which are formed by prompt coincident γ rays emitted by pairs of fragments or one fragment of a pair, and also γ rays emitted after fragment β decay. An example of a two-dimensional $\gamma-\gamma$ coincidence spectrum for the spontaneous fission of ^{252}Cf is shown in Fig. 1. Here we see that in addition to the peaks formed by the coincident γ rays when they are completely absorbed in the detector, the spectrum contains two series of background ridges parallel to the $E_{\gamma 1}$ and $E_{\gamma 2}$ axes. Each peak with energies $(E_{\gamma 1},E_{\gamma 2})$ is located at the intersection of two background ridges. The ridges are formed for coincident momenta of γ rays whose energy is completely absorbed in the germanium detectors and of incompletely absorbed γ rays or of γ rays of the quasicontinuous spectrum. The two-dimensional spectrum also includes a smooth background

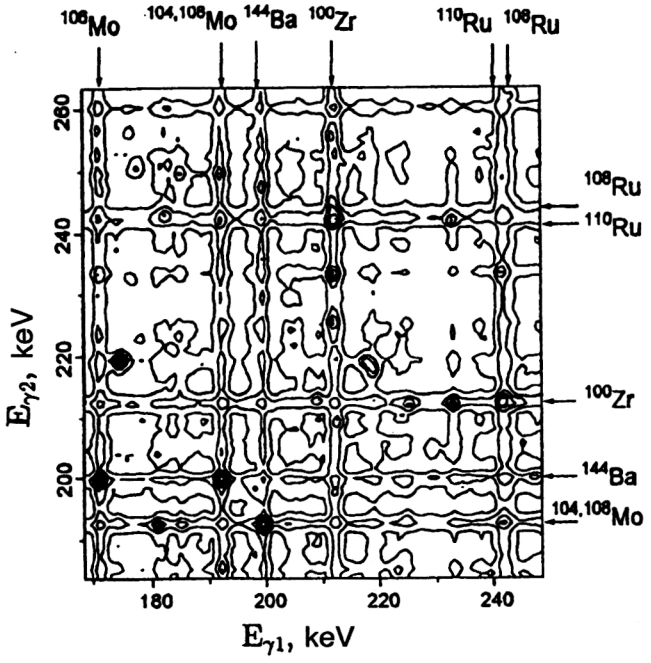

FIG. 1. Part of the two-dimensional $\gamma-\gamma$ coincidence spectrum (100×100 channels). The arrows indicate the energies of the γ rays corresponding to the $2^+\rightarrow 0^+$ transitions in various fragments.

produced by coincident γ rays whose energy is not completely resolved in the germanium detectors and γ rays of the quasicontinuous spectrum.

The background of any local region of the two-dimensional spectrum depends on the intensity and energy of γ transitions of higher energies, and also on the geometry of the detection system and the efficiency of the Compton shielding. To obtain the desired information it is important to correctly estimate the peak intensities in the two-dimensional $\gamma-\gamma$ coincidence spectrum. This requires the correct inclusion of both the smooth background and the ridge background.

Various methods of subtracting the background and estimating the peak intensities in coincidence γ spectra have been developed[100,101] to analyze the data obtained with 4π γ spectrometers and have been used successfully to construct nuclear level schemes. However, the methods of determining the peak intensity discussed in these studies are not accurate, owing to incomplete and incorrect background subtraction, as is noted by the authors themselves.

In this review we shall not give a detailed discussion of the construction of the background functions suggested in the studies mentioned above. Instead, we shall focus on one of the methods of processing the data on two-dimensional $\gamma-\gamma$ coincidence spectra most frequently used in nuclear spectroscopy. This is the analysis of the one-dimensional spectra obtained by superimposing "windows" on one of the energy axes of the two-dimensional spectrum $(E_{\gamma 1})$. A layer parallel to the second axis $E_{\gamma 2}$, with width equal to the energy window, is isolated from the two-dimensional spectrum. The one-dimensional spectrum is obtained as the projection of this layer on the $E_{\gamma 2}$ axis. The complete projections of the two-dimensional spectrum on the coordinate

axes are used as the background functions. The coefficient of a background function is defined as the ratio of the background intensity in the energy window to the total count in the projection of the two-dimensional spectrum. When this method is used to determine the intensities of peaks formed by coincident γ rays emitted from the same nucleus, the estimates obtained are not exact, but they do give reasonable results for the ratios of the intensities of these peaks. When the peaks in question are formed by γ rays emitted from different nuclei, the errors in estimating the intensities of these peaks can be large, and give incorrect results when the intensities of different peaks are compared.

It has been shown in Refs. 24, 25, and 102 that to obtain an accurate estimate of the peak intensities it is necessary to analyze the entire region of the two-dimensional spectrum near each peak studied. The authors of Ref. 102 proposed a method of background subtraction allowing accurate estimates of the peak intensity. The background functions are taken to be the projections of the spectrum in a small region near the peak in question which does not contain other peaks of comparable intensity. The peak intensity and coefficients of the background functions are found by fitting the data in this region of the spectrum. However, for the complicated spectra of coincident γ rays arising in the spontaneous fission of ^{252}Cf it is usually impossible to find a region free of peaks. Therefore, in Refs. 24 and 25 a different method[103,104] was used to correctly estimate the peak intensities. It amounts to approximating small segments of the two-dimensional spectrum by an analytic function.

To construct the approximating function it is necessary to find the coordinates of the maxima of all the possible peaks on the segment of interest of the two-dimensional spectrum. Accordingly, this segment of the two-dimensional spectrum is projected onto the coordinate axes. The locations of the maxima of all the peaks present are found in the one-dimensional projection spectra. If the shape of the spectra suggests that there are several superimposed lines in this region, these lines are separated and the coordinates of their maxima are also found. The peak shape is described by a Gaussian. We shall denote the peak centers and widths found in the one-dimensional convolutions as c_i and σ_i for $i=1,2,\ldots,m$ for the x ($E_{\gamma 1}$) axis, and d_j and σ_j for $j=1,2,\ldots,n$ for the y ($E_{\gamma 2}$) axis. The approximating function is the sum of three components, each corresponding to different components of the two-dimensional spectrum. The first component of this function describes the $\gamma-\gamma$ coincidence peaks:

$$\sum_{i=1}^{m}\sum_{j=1}^{m} A_{ij}\cdot\exp\left(-\frac{(x-c_i)^2}{2\sigma_i^2}-\frac{(y-d_j)^2}{2\sigma_j^2}\right).$$

The second component describes the background ridges:

$$\sum_{i=1}^{m} B_i\cdot\exp\left(-\frac{(x-c_i)^2}{2\sigma_i^2}\right)\sum_{j=1}^{n} H_j\cdot\exp\left(-\frac{(y-d_j)^2}{2\sigma_j^2}\right).$$

The third part of the function describes the smooth background:

$$k_1\cdot x+k_2\cdot y+k_3\cdot xy+k_4.$$

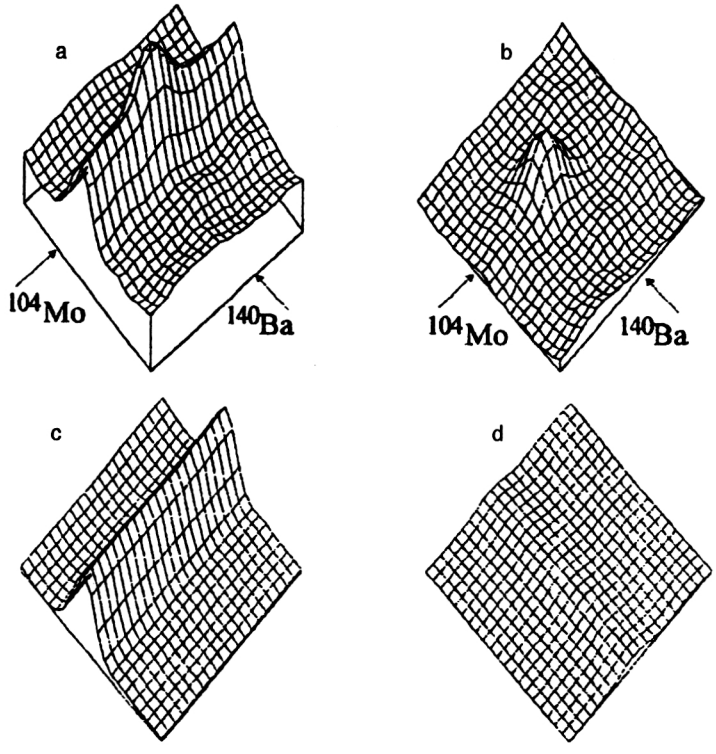

FIG. 2. (a) Part of the two-dimensional $\gamma-\gamma$ coincidence spectrum; (b) the spectrum after background subtraction; (c,d) the spectra of background ridges. The arrows indicate the energies of the γ rays corresponding to the $2^+\rightarrow 0^+$ transitions in ^{104}Mo and ^{140}Ba.

The free parameters of the approximating function A_{ij}, B_i, H_j, and k_l are determined by the least-squares method. In Fig. 2 we show an example of the background subtraction on a segment of the spectrum containing a peak formed by coincident γ rays of energies 192.2 keV and 602.3 keV, which correspond to $2^+\rightarrow 0^+$ transitions in ^{104}Mo and ^{140}Ba. The program FIT-2S was designed to search automatically for peaks and process the entire two-dimensional spectrum.[24,25] The program outputs a table of the coordinates and intensities of all the peaks found.

Various criteria can be used to establish the accuracy and reliability of the estimated peak intensities. First, the relative intensities of the γ transitions for various fragments can be compared with the analogous data in the literature, for example, for ^{100}Zr (Ref. 56), ^{148}Ce (Ref. 54), ^{136}Te (Ref. 59), and ^{144}Ba (Ref. 55).

Another criterion is to check the ratios of the intensities of coincident transitions which follow from the general properties of the γ cascade produced in the deexcitation of the fragment levels. It is known that for even–even fragments the γ cascade proceeds successively and corresponds to $E2$ transitions, the ground states of even–even nuclei have zero spin, and all the states of the rotational band have even spin. We shall use $(2n)^+$ to denote the state of a fragment level, and $(2n)^+\rightarrow(2n-2)^+$ to denote an $E2$ transition. Then the intensities of coincident transitions (with energies $E_{\gamma 1}$ and $E_{\gamma 2}$) of an even–even nucleus satisfy the relations

$$I(E_{(2k)^+\rightarrow(2k-2)^+}, E_{(2n)^+\rightarrow(2n-2)^+})=\text{const} \qquad (12)$$

for $k=\text{const}$ and $n=1,2,\ldots,k-1$, and

TABLE I. Independent yields of Ba–Mo fragment pairs in the spontaneous fission of ^{252}Cf. The yields are given as percentages.

	^{138}Ba	^{140}Ba	^{141}Ba	^{142}Ba	^{143}Ba	^{144}Ba	^{145}Ba	^{146}Ba	^{147}Ba	^{148}Ba
^{102}Mo			0.048(9)	0.04(2)	0.05(1)	0.07(1)	0.17(5)	0.13(4)	0.10(4)	0.09(4)
^{103}Mo		0.09(3)	0.14(8)	0.08(3)	0.12(8)	0.63(8)	1.3(3)	0.50(6)	0.36(5)	0.15(9)
^{104}Mo	0.07(3)	0.13(4)	0.21(9)	0.32(4)	0.45(7)	1.00(8)	0.84(9)	0.33(3)	0.13(7)	0.05(2)
^{105}Mo		0.10(3)	0.10(3)	0.58(7)	1.16(13)	1.2(1)	0.78(15)	0.12(5)	0.2(1)	
^{106}Mo		0.12(2)	0.35(7)	0.91(8)	1.0(1)	0.58(4)	0.15(6)	0.04(3)		
^{107}Mo		0.10(3)	0.14(3)	0.32(3)	0.37(5)	0.14(5)	0.10(5)			
^{108}Mo		0.10(2)	0.11(3)	0.13(5)	0.16(4)	0.08(5)				

$$I(E_{(2k)^+\to(2k-2)^+},E_{2^+\to0^+})/I(E_{(2k)^+\to(2k-2)^+},E_{4^+\to2^+})=1 \quad (13)$$

for $k>2$.

Yet another method of judging the accuracy of the estimated peak intensities is to check that zero is obtained for the intensities of peaks corresponding to γ rays from fragments for which the sum of the nuclear charges is not equal to the charge of the fissioning nucleus ($Z_1+Z_2\neq Z_F$) or for which the sum of the mass numbers is larger ($A_1'+A_2'>A_F$) or significantly smaller ($A_1'+A_2'<A_F-11$) than the mass of the fissioning nucleus. This check also allows evaluation of the probability of observing triple fission.

The use of these criteria together with the method of determining the peak intensities[24,25] results in good estimates whose accuracy is mainly determined by the statistical error.

2.2. The fragment-pair yields

The study of coincident γ rays emitted from the two fission fragments allows a new type of data to be obtained: the fragment-pair yields. In Refs. 24, 25, 29, and 30 the yields of ~150 pairs of fragments were determined. They correspond to five charge splits of ^{252}Cf:

$Z_1/Z_2=46/52$ (Pd–Te) 44/54 (Ru–Xe),

42/56 (Mo–Ba), 40/58 (Zr–Ce),

38/60 (Sr–Nd).

The relative yields of fragment pairs with even mass numbers were determined from the intensity of $\gamma-\gamma$ coincidences due to γ transitions from the low-lying 2^+ level to the 0^+ ground state in each nucleus. When one of the fragments of the pair had odd mass number, the fragment-pair yield was found from the sum of the intensities of $\gamma-\gamma$ coincidences produced by the $2^+\to0^+$ γ transition in the A-even fragment and all the γ transitions to the ground state in the A-odd fragment. When the two fragments were both A-odd, the sum of the intensities of $\gamma-\gamma$ coincidences over all possible combinations of γ transitions to the ground state in each fragment was used. The intensity of $\gamma-\gamma$ coincidences was determined from the intensity of the corresponding peaks in the two-dimensional spectrum after taking into account the detector efficiency in recording γ rays and the probability of internal conversion of nuclear levels.

The relative yields of fragment pairs thus found were converted into independent yields as a result of normalization using the data in the literature on the independent yields of certain nuclei in the spontaneous fission of ^{252}Cf (Ref. 60). As an example, in Table I we give the independent yields of fragment pairs for the Ba–Mo division of ^{252}Cf. Analogous data on the fragment-pair yields were also obtained for the Te–Pd, Xe–Ru, Ce–Zr, and Nd–Sr divisions of ^{252}Cf.

The tables of fragment-pair yields can be used to obtain some integrated characteristics of nuclear fission. By adding the yields of pairs containing fragments with mass number A_1' and charge Z_1, it is possible to determine the yield of a given fragment $Y(Z_1,A_1')$ in nuclear fission. The yields of various isotopes of barium and molybdenum can be obtained from Table I by adding the yields of fragment pairs in rows and columns, respectively. The resulting isotopic distributions for ten elements are shown in Fig. 3. The independent yields of various isotopes given in this figure agree fairly well with the analogous calculated data.[105]

Each observed fragment pair is formed after the evaporation of a certain number of prompt neutrons from the primary fragments, $\nu_{tot}=A_F-A_1'-A_2'$. Therefore, by summing

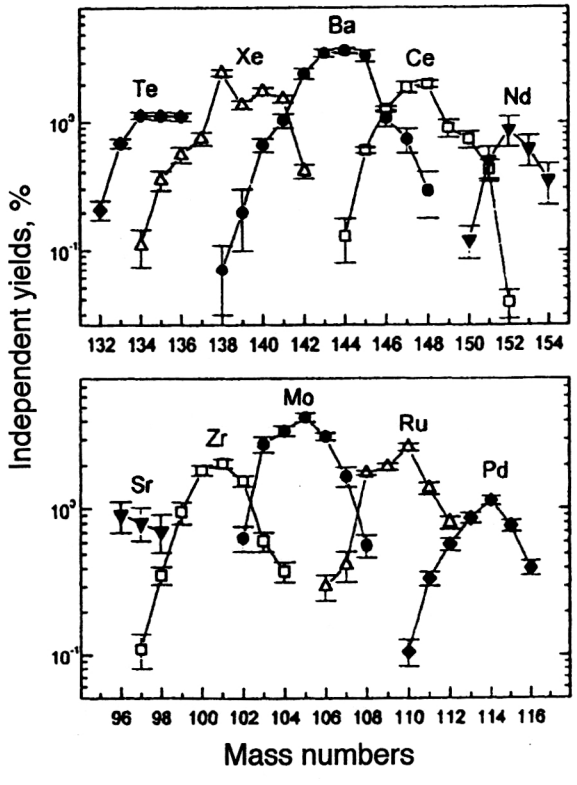

FIG. 3. Isotopic distributions of fragments from the spontaneous fission of ^{252}Cf.

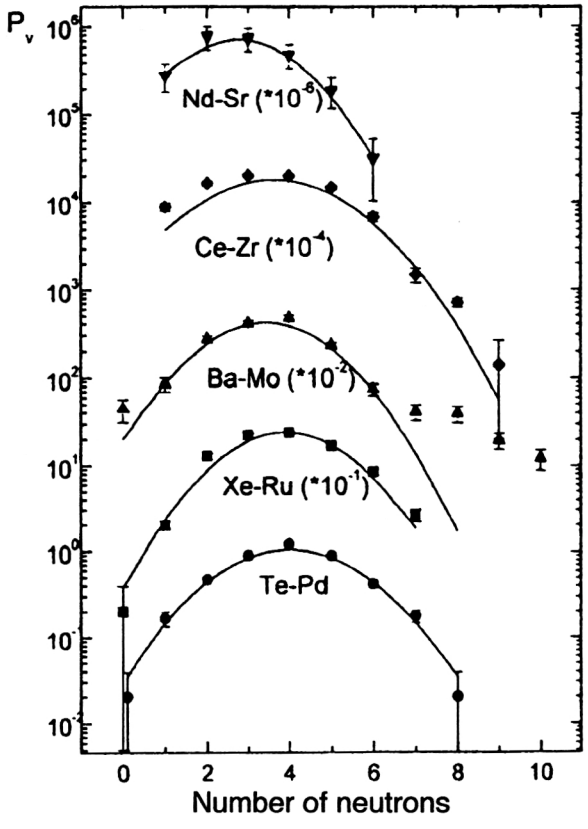

FIG. 4. Neutron multiplicity distributions for five charge splits of ^{252}Cf. The lines show the results of approximating the experimental points by Gaussians. The neutron evaporation probabilities (P_ν) multiplied by the coefficients shown in the figure give the neutron yields in percent per fission.

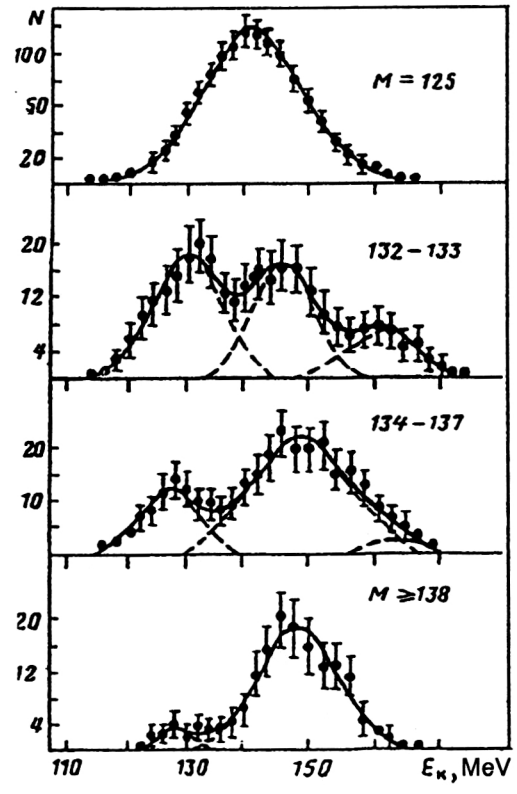

FIG. 5. Kinetic-energy distributions of fission fragments of ^{213}At for selected mass ranges of the fragments (Ref. 9).

the fragment-pair yields corresponding to the emission of 0, 1, 2, etc., neutrons it is possible to obtain the neutron multiplicity distributions for various values of the nuclear charges of the fragments. In Fig. 4 we give the neutron multiplicity distributions for five charge splits of ^{252}Cf. For four of the charge splits the experimental points are described well by Gaussians. The Ba–Mo split differs from the others in having a higher yield of fragment pairs formed after the evaporation of seven or more neutrons. This feature of the Ba–Mo split is manifested clearly in the neutron multiplicity distribution. We see from Fig. 4 that in addition to the component present in the neighboring splits, the Ba–Mo split contains a second component with average neutron multiplicity equal to 8.

The two components observed in the neutron multiplicity distribution of the Ba–Mo division suggest the presence of two fission modes for this charge asymmetry of the ^{252}Cf fission fragments. In fact, the different fission modes are distinguished by the nuclear configurations at the breakup point. Each fission mode has a distribution of configurations about the most probable nuclear shape, which is characterized by the mass asymmetry and deformation (i.e., the distance between the fragment centers) of the produced fragments. Bimodal nuclear fission has been discovered and studied experimentally, and the mass distributions and total kinetic-energy distributions of the fission fragments have been measured.[9,106] The fragment mass distributions and kinetic-energy spectra for each fission mode are described well by Gaussians. A sign of the presence of two (or more) fission modes is the observation of two (or several) components in the experimental mass and energy spectra, i.e., the possibility of describing the experimental spectra by a superposition of Gaussians. The best resolution of fission modes can be obtained by observing the fragment mass spectra for various fixed values of the kinetic energy or the kinetic-energy spectra at fixed values of the fragment masses. The asymmetric fission modes of preactinide nuclei have been observed in this way.[9] In Fig. 5 we show the experimental kinetic-energy spectra of fragments from the fission of ^{213}At for various mass ranges, taken from Ref. 9. A special feature of the method based on measurements of the fragment-pair yields is the fact that bimodal fission has been observed in the neutron multiplicity spectra for various values of the fragment charges (see Fig. 4).

Pairs of secondary fragments are formed as a result of the deexcitation of primary fragments, and therefore the tables of pair yields obtained for secondary fragments contain information about the mass and energy distributions of the primary fragments. In Refs. 24, 25, and 30 the pair yields of secondary fragments were used to reconstruct the parameters of the mass and energy distributions of the primary fragments: Xe–Ru, Ba–Mo, and Ce–Zr. The analysis was performed by assuming that the distributions of the primary fragments in mass, excitation energy, and total kinetic energy for a fixed charge split are Gaussians for each fission mode. The experimental data for the Xe–Ru and Ce–Zr splits are described well by a single fission mode, while for the Ba–Mo split two modes are needed. The first fission

mode for the Ba–Mo split had an ordinary value of the total fragment kinetic energy $\overline{\text{TKE}}_1 = 189$ MeV. A considerably smaller value of the total fragment kinetic energy was obtained for the second mode: $\overline{\text{TKE}}_2 = 154$ MeV. The second fission mode gives the dominant contribution to the production of very light pairs of secondary Ba–Mo fragments.

Important characteristics of fission like the average value of the total kinetic energy ($\overline{\text{TKE}}$) and the spread of the total kinetic-energy distribution (σ_{TKE}) for the three charge splits Xe–Ru, Ba–Mo, and Ce–Zr found in the analysis agree fairly well with the analogous data obtained in direct measurements of the fragment kinetic energies.[31,90] The characteristics of the mass distributions of primary fragments $\bar{A}(Z)$ and σ_A obtained in Refs. 24, 25, and 30 agree well with the results of calculations based on the analysis of completely different experimental data: the cumulative, fractional, and independent yields of fragments in the spontaneous fission of ^{252}Cf (Ref. 105).

Thus, data on the fragment-pair yields allow study of the characteristics of the primary fission fragments produced immediately after the breakup of the nucleus.

2.3. The angular momenta of the fragments of spontaneous fission of ^{252}Cf

The observation of the coincident γ rays emitted from two simultaneously produced fission fragments makes it possible to obtain data characterizing the fragment angular momenta in more detail than by the other methods of study used earlier. It is possible to measure experimentally the intensities of γ transitions between different excited states for a fragment of charge Z_1 and mass A_1' when this fragment is formed as part of a pair with another fragment having known charge $Z_2 = Z_F - Z_1$ and mass $A_2' = A_F - A_1' - \nu_{\text{tot}}$, where ν_{tot} is the total number of neutrons evaporated from the primary fragments in the formation of the fragment pair in question. That is, for a fragment with definite Z and A' one measures the intensities of γ transitions when this fragment is formed as a result of the evaporation of a certain number of neutrons ν_{tot}.

The measured intensities of γ transitions between different excited states can be used to find the probabilities of populating these states in fission. The population probability of a state P_i is found as the difference between the summed intensities $I_{k\to i}$ of all transitions to this state and the summed intensities $I_{i\to l}$ of all transitions from this state:

$$P_i = R \cdot \Delta I_i = R \cdot \left(\sum_k I_{k\to i} - \sum_l I_{i\to l} \right),$$

where the normalization factor R is defined as $R = 1/\Sigma_i \Delta I_i$.

The values found for the P_i and the known spins of the states J_i can be used to find the average value of the angular momentum for the fragment in question:

$$\bar{J}_\gamma = \frac{\Sigma_i P_i \cdot J_i}{\Sigma_i P_i}.$$

Even–even fragments were studied in Refs. 28 and 30, because it is for them that the schemes of levels populated in fission have been most thoroughly studied. For a given fragment produced as part of a pair with another having even mass number, the γ-transition intensity was determined from the intensity of coincidences due to the γ transition in the nucleus in question and the $2^+ \to 0^+$ transition in the other fragment. When the other fragment had odd mass number, the sum of the intensities of coincidences due to the γ transition in the nucleus in question and all transitions to the ground state in the other fragment was used.

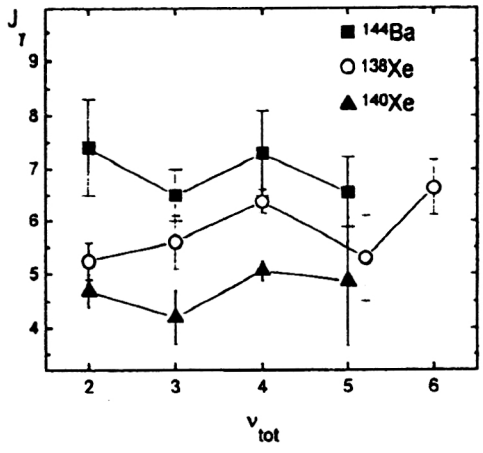

FIG. 6. Dependence of the angular momenta of the fragments ^{144}Ba, ^{138}Xe, and ^{140}Xe on the total number of neutrons ν_{tot} evaporated from the primary fragments in the formation of these isotopes.

The γ-transition intensities, the level population probabilities, and the average angular momenta were found for ^{144}Ba, ^{138}Xe, and ^{140}Xe when these fragments are produced in pairs with different isotopes, respectively, Mo and Ru, as a result of the evaporation of different numbers of neutrons (from 2 to 6 neutrons). The ν_{tot} dependences of the average angular momentum for ^{144}Ba, ^{138}Xe, and ^{140}Xe are shown in Fig. 6. For these heavy fragments the value of $\bar{J}_\gamma$ varies little with varying number of evaporated neutrons. However, if the angular momentum carried off by the evaporated neutrons is taken into account, the values of $\bar{J}_\gamma$ obtained suggest that the angular momentum of the primary fragments Xe and Ba grows with increasing excitation energy, which is consistent with the conclusions of theoretical[19,20] and experimental[107,108] studies.

An unusual dependence of the angular momentum of the primary fragments was obtained in studying pairs of fragments produced by ^{104}Mo and various isotopes of barium after the evaporation of from 0 to 10 neutrons.[28,30] The ν_{tot} dependences of $\bar{J}_\gamma$ for ^{104}Mo and even isotopes of barium produced in pairs with ^{104}Mo are shown in Figs. 7a and 7b, respectively. Here we see that the angular momenta of the studied fragment pairs increase as the number of neutrons varies from 0 to 5, and then they decrease as the number of evaporated neutrons increases further. In Fig. 7c we give the total angular momenta of primary Ba–Mo fragment pairs obtained taking into account the angular momentum carried off by the neutrons. The angular momentum of the primary Ba–Mo fragment pairs grows as the neutron multiplicity increases from 0 to 4, then as the number of evaporated neutrons increases further we observe anomalous behavior of the fragment angular momentum: as the number of evaporated

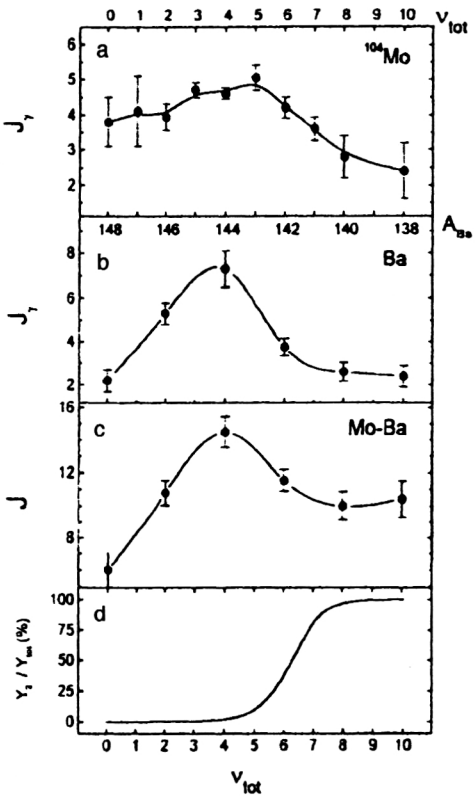

FIG. 7. Dependence on the total number of neutrons of (a) the angular momenta of ^{104}Mo fragments; (b) the angular momenta of Ba fragments produced in pairs with ^{104}Mo; (c) the total angular momenta of primary Ba–Mo fragment pairs; (d) the relative contribution of the second fission mode to the production of Ba–^{104}Mo fragment pairs.

neutrons, i.e., the fragment excitation energy, increases, the fragment angular momentum does not grow. This behavior of the angular momentum can be attributed to the presence of two fission modes and to the differences between these modes in the excitation of collective degrees of freedom in the fissioning nucleus. In Fig. 7d we show the relative contribution of the second fission mode to the production of the Ba–Mo fragment pairs obtained by analyzing the yields of pairs of secondary fragments.[24,25] Here we see that the falloff of the fragment angular momentum $\bar{J}_{\gamma Mo}$ and $\bar{J}_{\gamma Ba}$ and the anomalous behavior of the angular momenta of the primary fragments is correlated with the contribution of the second mode in the production of the Ba–Mo pairs in question.

2.4. Conclusion

The method of studying nuclear fission based on the spectrometry of multiple fission γ rays allows the determination of new detailed characteristics of fission: the fragment-pair yields and the population probabilities of the excited levels of the fragments making up these pairs. These experimental data lead directly to integral fission characteristics, which have also been obtained for the first time. These are the neutron multiplicity distributions for various charge splits of the fissioning nucleus and the dependence of the angular momenta of the individual fragments on the number of evaporated neutrons. The experimental data contain information about the charges, masses, excitation energies, and spins of pairs of fission fragments. Experiments in which the new method of studying fission is combined with traditional methods such as measurement of the velocities and/or kinetic energies of the two fragments appear promising for the study of nuclear fission, since they would provide data giving the most complete characterization of nuclear fission. The new method can also be used to study both spontaneous fission and the low-energy fission of various nuclei.

[1] *The Nuclear Fission Process*, edited by C. Wagemans (CRC Press, Boca Raton, Florida, 1991).
[2] V. V. Pashkevich, Nucl. Phys. A **161**, 275 (1971).
[3] J. F. Berger, M. Girod, and D. Gogny, in *Proceedings of the Conf. "Fifty Years of Research in Nuclear Fission,"* Berlin, 1989; Nucl. Phys. A **502**, 85c (1989).
[4] U. Brosa, S. Grossman, and A. Müller, Z. Naturforsch. **41a**, 1341 (1986).
[5] P. Möller, J. R. Nix, and W. J. Swiatecki, Nucl. Phys. A **492**, 348 (1989).
[6] S. Cwiok, P. Rozmej, A. Sobiczewski, and Z. Patyk, Nucl. Phys. A **491**, 281 (1989).
[7] H.-H. Knitter *et al.*, Z. Naturforsch. **42a**, 786 (1987).
[8] D. C. Hoffman, in *Proceedings of the Conf. "Fifty Years of Research in Nuclear Fission,"* Berlin, 1989; Nucl. Phys. A **502**, 21c (1989).
[9] M. G. Itkis *et al.*, Fiz. Élem. Chastits At Yadra **19**, 701 (1988) [Sov. J. Part. Nucl. **19**, 301 (1988)].
[10] U. Brosa, S. Grossman, and A. Müller, Phys. Rep. **197**, 167 (1990).
[11] J. P. Bocquet and R. Brissot, in *Proceeding of the Conf. "Fifty Years of Research in Nuclear Fission,"* Berlin, 1989; Nucl. Phys. A **502**, 213c (1989).
[12] M. Berlanger, A. Gobbi, F. Hanappe *et al.*, Z. Phys. A **291**, 133 (1979).
[13] H. A. Nifenecker, J. Phys. Lett. **41**, 47 (1980).
[14] N. Boucheneb, P. Geltenbort, M. Asghar *et al.*, Nucl. Phys. A **502**, 261c (1989).
[15] M. Djebara, M. Asghar, J. P. Bocquet *et al.*, Nucl. Phys. A **496**, 346 (1989).
[16] H. A. Nifenecker, G. Mariolopoulos, J. P. Bocquet *et al.*, Z. Phys. A **308**, 39 (1982).
[17] G. Gönnenwein, in *Proceedings of the Intern. Conf. "Fiftieth Anniversary of Nuclear Fission,"* Leningrad, 1989 (Khlopin Institute, St. Petersburg, 1992), Vol. 1, p. 182.
[18] J. P. Bocquet, H. R. Faust, M. Fowler *et al.*, Z. Phys. A **335**, 41 (1990).
[19] J. O. Rasmussen, W. Nörenberg, and H. H. Mang, Nucl. Phys. A **136**, 465 (1969).
[20] M. Zielinska-Pfabe and K. Dietrich, Phys. Rev. B **49**, 123 (1974).
[21] J. H. Hamilton *et al.*, in *Proceedings of the Intern. School-Seminar on Heavy Ion Physics*, Dubna, Russia, 1993, edited by Yu. Ts. Oganessian, Yu. E. Penionzhkevich, and R. Kalpakchieva (JINR, Dubna, 1993), Vol. 1, p. 276.
[22] J. H. Hamilton, G. M. Ter-Akopian, Yu. Ts. Oganessian *et al.*, in *Proceedings of the Conf. on Low Energy Nuclear Dynamics (LEND '95)*, St. Petersburg (World Scientific, Singapore, 1995), p. 187.
[23] J. H. Hamilton *et al.*, Prog. Part. Nucl. Phys. **35**, 635 (1995).
[24] G. M. Ter-Akopian, J. H. Hamilton, Yu. Ts. Oganessian *et al.*, in *Proceedings of the Conf. on Exotic Nuclei and Atomic Masses (ENAM 95)*, edited by M. de Saint Simon and X. Sorlin (Editions Frontières, Gif-sur-Yvette, 1995), p. 383.
[25] G. M. Ter-Akop'yan *et al.*, in *Proceedings of the Meeting on Nuclear Spectroscopy and Nuclear Structure*, St. Petersburg, 1995; Izv. Ross. Akad. Nauk, Ser. Fiz. **60**, 162 (1996) [Bull. Russ. Acad. Sci., Phys. Ser.].
[26] G. M. Ter-Akopian *et al.*, Phys. Rev. Lett. **73**, 1477 (1994).
[27] G. M. Ter-Akopian *et al.*, Phys. Rev. Lett. **77**, 32 (1996).
[28] G. M. Ter-Akopian *et al.*, in *Proceedings of the Meeting on Nuclear Spectroscopy and Nuclear Structure*, Moscow, 1996; Izv. Ross. Akad. Nauk, Ser. Fiz. **61**, 194 (1997) [Bull Russ. Acad. Sci., Phys. Ser.].
[29] G. M. Ter-Akopian *et al.*, in *Proceedings of the Meeting on Nuclear Spectroscopy and Nuclear Structure*, Moscow, 1996; Izv. Ross. Akad. Nauk, Ser. Fiz. **61**, 747 (1997) [Bull. Russ. Acad. Sci., Phys. Ser.].
[30] G. M. Ter-Akopian *et al.*, Phys. Rev. C **55**, 1146 (1997).
[31] C. Budtz-Jørgensen and H.-H. Knitter, Nucl. Phys. A **490**, 307 (1988).
[32] R. L. Watson, J. B. Wilhelmy, R. C. Jared *et al.*, Nucl. Phys. A **141**, 449 (1970).
[33] J. Terrell, Phys. Rev. **127**, 880 (1962).
[34] H. W. Schmitt, W. M. Gibson, J. H. Neiler *et al.*, in *Proceedings of the*

Symp. on the Physics and Chemistry of Fission (IAEA, Vienna, 1965), Vol. 1, p. 531.
[35] E. Weissenberger, P. Geltenbort, A. Oed *et al.*, Nucl. Instrum. Methods Phys. Res. A **248**, 506 (1986).
[36] D. W. Lang and R. L. Walsh, Nucl. Instrum. Methods Phys. Res. **200**, 389 (1982).
[37] V. A. Khryachkov *et al.*, in *Proceedings of the Intern. Conf. "Nuclear Fission—50 Years,"* Leningrad, 1989; St. Petersburg, 1992, Vol. 2, p. 454 [in Russian].
[38] C. Budtz-Jørgensen *et al.*, Nucl. Instrum. Methods Phys. Res. A **258**, 209 (1987).
[39] A. Oed, P. Geltenbort, F. Gönnenwein, T. Manning, and D. Souque, Nucl. Instrum. Methods Phys. Res. A **205**, 455 (1983).
[40] C. Signarbieux *et al.*, J. Phys. Lett. (Paris) **46**, L1095 (1985).
[41] F.-J. Hambsch, H.-H. Knitter, and C. Budtz-Jørgensen, Nucl. Phys. A **554**, 209 (1993).
[42] V. A. Khryachkov *et al.*, Yad. Fiz. **53**, 621 (1991) [Sov. J. Nucl. Phys. **53**, 387 (1991)].
[43] A. Oed, P. Geltenbort, R. Brissot *et al.*, Nucl. Instrum. Methods Phys. Res. A **219**, 569 (1984).
[44] A. Oed *et al.*, Nucl. Instrum. Methods **179**, 71 (1981).
[45] F. Gönnenwein, Nucl. Phys. A **502**, 159c (1989).
[46] W. Reisdorf, J. P. Unik, H. C. Griffin, and L. E. Glendenin, Nucl. Phys. A **177**, 337 (1971).
[47] H. A. Nifenecker, J. Blachot, J. P. Bocquet *et al.*, in *Proceedings of the Symp. on the Physics and Chemistry of Fission*, Jülich, 1979 (IAEA, Vienna, 1980), Vol. 2, p. 35.
[48] P. J. Nolan, F. A. Beck, and G. Siegert, Ann. Rev. Nucl. Part. Sci. **45**, 561 (1994).
[49] R. Aryaeinejad *et al.*, Phys. Rev. C **48**, 566 (1993).
[50] K. Buttler-Moore, J. H. Hamilton, A. V. Ramayya *et al.*, J. Phys. G **19**, L121 (1993).
[51] K. Buttler-Moore, R. Aryaeinejad, J. D. Cole *et al.*, Phys. Rev. C **52**, 1339 (1995).
[52] Q. H. Lu, K. Buttler-Moore, S. J. Zhu *et al.*, Phys. Rev. C **52**, 1348 (1995).
[53] S. J. Zhu, Q. H. Lu, J. H. Hamilton *et al.*, Phys. Lett. B **357**, 273 (1995).
[54] W. R. Phillips *et al.*, Phys. Lett. B **212**, 402 (1988).
[55] W. R. Phillips *et al.*, Phys. Rev. Lett. **57**, 3257 (1986).
[56] M. A. C. Hotchkis, J. L. Durell, J. B. Fitzgerald *et al.*, Nucl. Phys. A **530**, 111 (1991).
[57] A. S. Mawbray *et al.*, Phys. Rev. C **42**, 1126 (1990).
[58] M. A. C. Hotchkis *et al.*, Phys. Rev. Lett. **64**, 2123 (1990).
[59] J. A. Cizewski *et al.*, Phys. Rev. C **47**, 1294 (1993).
[60] E. Cheifetz, J. B. Wilhelmy, R. C. Jared, and S. G. Thompson, Phys. Rev. C **4**, 1913 (1971).
[61] A. A. Bogdzel' *et al.*, Report R3-87-862, JINR, Dubna (1987) [in Russian].
[62] N. A. Gundorin *et al.*, Report R15-94-526, JINR, Dubna (1994) [in Russian].
[63] U. Quade, K. Rudolph, and G. Siegert, Nucl. Instrum. Methods A **164**, 435 (1979).
[64] H. G. Clerc *et al.*, Nucl. Instrum. Methods A **124**, 607 (1975).
[65] G. Siegert, H. Wollnik, J. Greif *et al.*, Phys. Lett. B **53**, 45 (1974).
[66] J. P. Bocquet, R. Brissot, and H. R. Faust, Nucl. Instrum. Methods Phys. Res. A **267**, 466 (1988).
[67] C. Budtz-Jørgensen, H.-H. Knitter, Ch. Straede *et al.*, Nucl. Instrum. Methods Phys. Res. A **258**, 209 (1987).
[68] K. Skarsvag, Nucl. Phys. A **253**, 274 (1975)
[69] J. W. Boldeman, Nucl. Data Standards for Nucl. Measurements, 1992, p. 108.
[70] E. E. Maslin *et al.*, Phys. Rev. **164**, 1520 (1965).
[71] J. W. Boldeman *et al.*, Aust. J. Phys. **24**, 821 (1971).
[72] R. Müller *et al.*, Phys. Rev. C **29**, 885 (1984).
[73] V. F. Apalin *et al.*, Nucl. Phys. **71**, 533 (1965).
[74] J. F. Wild, J. van Aarle, W. Westmeier *et al.*, Phys. Rev. C **41**, 640 (1990).
[75] C. Signarbieux, R. Babinet, H. Nifenecker, and J. Poitou, in *Proceedings of the Symp. on the Physics and Chemistry of Fission* (IAEA, Vienna, 1974), Vol. 2, p. 179.
[76] R. L. Walsh and J. W. Boldeman, Nucl. Phys. A **276**, 189 (1977).
[77] H. R. Bowman, J. C. D. Milton, S. G. Thompson, and W. J. Swiatecki, Phys. Rev. **129**, 2133 (1963).
[78] R. Schmidt and H. Henschel, Nucl. Phys. A **395**, 29 (1983).
[79] I. D. Alkhazov, B. F. Gerasimenko, A. V. Kuznetsov *et al.*, Yad. Fiz. **48**, 1635 (1988) [Sov. J. Nucl. Phys. **48**, 978 (1988)].
[80] J. Van Aarle, W. Westmeier, R. A. Esterlund, and P. Patzelt, Nucl. Phys. A **578**, 77 (1994).
[81] J. Grindler, Phys. Rev. C **19**, 1806 (1979).
[82] J. C. Milton and J. S. Fraser, in *Proceedings of the Symp. on the Physics and Chemistry of Fission* (IAEA, Vienna, 1965), Vol. 2, p. 39.
[83] U. Jahke *et al.*, in *Proceedings of the Symp. on Detectors in Heavy-Ion Reactions*, Lecture Notes in Physics, Vol. 178, p. 179 (1983).
[84] D. Habs *et al.*, in *Proceedings of the Symp. on Detectors in Heavy-Ion Reactions*, Lecture Notes in Physics, Vol. 178, p. 163 (1983).
[85] P. Glässel *et al.*, Nucl. Phys. A **502**, 315c (1989).
[86] H. W. Schmitt, R. W. Lide, and F. Pleasonton, Nucl. Instrum. Methods **63**, 237 (1968).
[87] W. E. Stein, in *Proceedings of the Symp. on the Physics and Chemistry of Fission* (IAEA, Vienna, 1965), Vol. 1, p. 491.
[88] Y. Nakagome, I. Kanno, and I. Kimura, in *Proceedings of 50 Years With Nuclear Fission*, Washington, 1989, Vol. 1, p. 360.
[89] P. Möller and J. R. Nix, At. Data Nucl. Data Tables **26**, 165 (1981).
[90] H. Nifenecker, C. Signarbieux, R. Babinet, and J. Poitou, in *Proceedings of the Symp. on the Physics and Chemistry of Fission*, Rochester, 1973 (IAEA, Vienna, 1974), Vol. 2, p. 117.
[91] J. R. Nix and W. J. Swiatecki, Nucl. Phys. **71**, 1 (1965).
[92] V. M. Strutinskiĭ, Zh. Éksp. Teor. Fiz. **39**, 781 (1960) [Sov. Phys. JETP **12**, 546 (1961)].
[93] H. Nifenecker, C. Signarbieux, M. Ribrag *et al.*, Nucl. Phys. A **189**, 285 (1972).
[94] D. G. Sarantites, G. E. Gordon, and C. D. Coryell, Phys. Rev. **138**, B353 (1965).
[95] H. Naik, S. P. Dange, R. J. Singh, and T. Datta, Nucl. Phys. A **587**, 273 (1995).
[96] D. De Frenne, in *The Nuclear Fission Process*, edited by C. Wagemans (CRC Press, Boca Raton, 1991), p. 476.
[97] J. R. Huizenga and R. Vandenbosch, Phys. Rev. **120**, 1305 (1960).
[98] R. Vandenbosch and J. R. Huizenga, Phys. Rev. **120**, 1313 (1960).
[99] J. B. Wilhelmy *et al.*, Phys. Rev. C **5**, 2041 (1972).
[100] D. C. Radford, Nucl. Instrum. Methods Phys. Res. A **361**, 306 (1995).
[101] D. C. Radford, Nucl. Instrum. Methods Phys. Res. A **361**, 297 (1995).
[102] A. G. Smith and W. J. Vermeer, Nucl. Instrum. Methods Phys. Res. A **350**, 314 (1994).
[103] D. A. Emellanov *et al.*, Nucl. Instrum. Methods **178**, 555 (1980).
[104] F. Bulla *et al.*, Report R10-80-104, JINR, Dubna (1980) [in Russian].
[105] A. C. Wahl, At. Data Nucl. Data Tables **39**, 1 (1988).
[106] E. K. Hulet *et al.*, Phys. Rev. Lett. **56**, 313 (1986).
[107] H. O. Densschlag *et al.*, in *Proceedings of the Symp. on the Physics and Chemistry of Fission* (IAEA, Vienna, 1980), Vol. 2, p. 153.
[108] J. P. Bocquet *et al.*, in *Proceedings of the Symp. on the Physics and Chemistry of Fission* (IAEA, Vienna, 1980), Vol. 2, p. 179.

Translated by Patricia A. Millard